JCTC Journal of Chemical Theory and Computation

The B(OH)−NH Analog Is a Surrogate for the Amide Bond (CO−NH) in Peptides: An ab Initio Study

Alpeshkumar K. Malde, Santosh A. Khedkar, and Evans C. Coutinho*

Department of Pharmaceutical Chemistry, Bombay College of Pharmacy, Kalina, Santacruz (E), Mumbai 400 098, India

Received August 7, 2006

Abstract: The conformational preferences of *N*-methyl-methylboronamide (NMB), a B(OH)−NH analog of the amide CO−NH in natural peptides, have been investigated at the Hartree−Fock; Becke's three-parameter exchange functional and the gradient-corrected functional of Lee, Yang, and Parr; and second-order Møller−Plesset levels of theory with the 6-31+G* basis set. The minima, saddle points, and rotation barriers on the potential energy surface of NMB have been located and the energy barriers estimated. Besides the global minimum, there are three local minima within 2.0 kcal mol^{-1} of the global minimum characterized by specific ω and τ torsion values. The energy barriers for rotation about the "ω angle" are 16.4−18.8 kcal mol^{-1} and are a consequence of the double-bond character of the B−N bond as revealed by natural bond orbitals calculations. The "ω angle" and the ω rotation barrier are nearly the same as those seen in natural peptides. The τ rotation barriers (B−O bond) are relatively low because of the single-bond character of the B−O bond. Ala-BON, the Ala-dipeptide derived from NMB, has been constructed as a model peptide to study the conformational preferences about the ϕ and ψ torsion angles. The study reveals a strong preference for α-helix, type-II β-turn, 2.27 ribbon, and antiparallel β-sheet conformations, and mirror images of both type-II β-turn and 2.27 ribbon motifs whose ϕ and ψ values fall in the "disfavored regions" of the Ramachandran map. Thus, the replacement of the carbonyl group by B−OH retains the geometry and barrier around the "ω angle" and induces a strong preference for regular secondary structure motifs and also structures with positive ϕ values. This makes the B(OH)−NH analog an important surrogate for the peptide bond, with the additional advantage of stability to proteolytic enzymes.

Introduction

The building blocks of most of the peptides and proteins are the 20 naturally occurring amino acids. Extensive experimental and theoretical studies have been carried out to understand the chemical and physical properties of these molecules. The use of physiologically relevant peptides in therapeutics is often hampered by their poor oral bioavailability.[1] Moreover, the pharmacological use of peptides or any drug demands high potency, good selectivity and specificity, metabolic stability, and low toxicity.[2] To achieve these demands, numerous modifications of the amino acid backbone and side chains have been suggested over the years. Side-chain modifications include the inversion of chirality of one or more key residues in the peptide,[3] introduction of a double bond between the Cα and Cβ atoms,[4] and moving the side chain from the Cα position to the N atom to form peptoids.[5] Some of the backbone modifications include elongation with β-, γ-, and δ-amino acids;[6] replacement of the amide bond[7] by sulfonamide, phosphonamidate, and carbamate; reduction of the amide bond;[8] *N*-methylation;[9] *N*-hydroxylation;[10] isosteric replacement of Cα by boron forming amino-carboxyboranes;[11] replacement of the amide NH by BH,[12,13] BOH,[14] or $BOCH_3$,[15] and replacement of the carbonyl carbon with boron, forming peptide boronic acid.[16]

* Corresponding author tel.: +91-22-26670871; fax: +91-22-26670816; e-mail: evans@bcpindia.org.

10.1021/ct600256s CCC: $37.00
Published on Web 12/22/2006

Chart 1

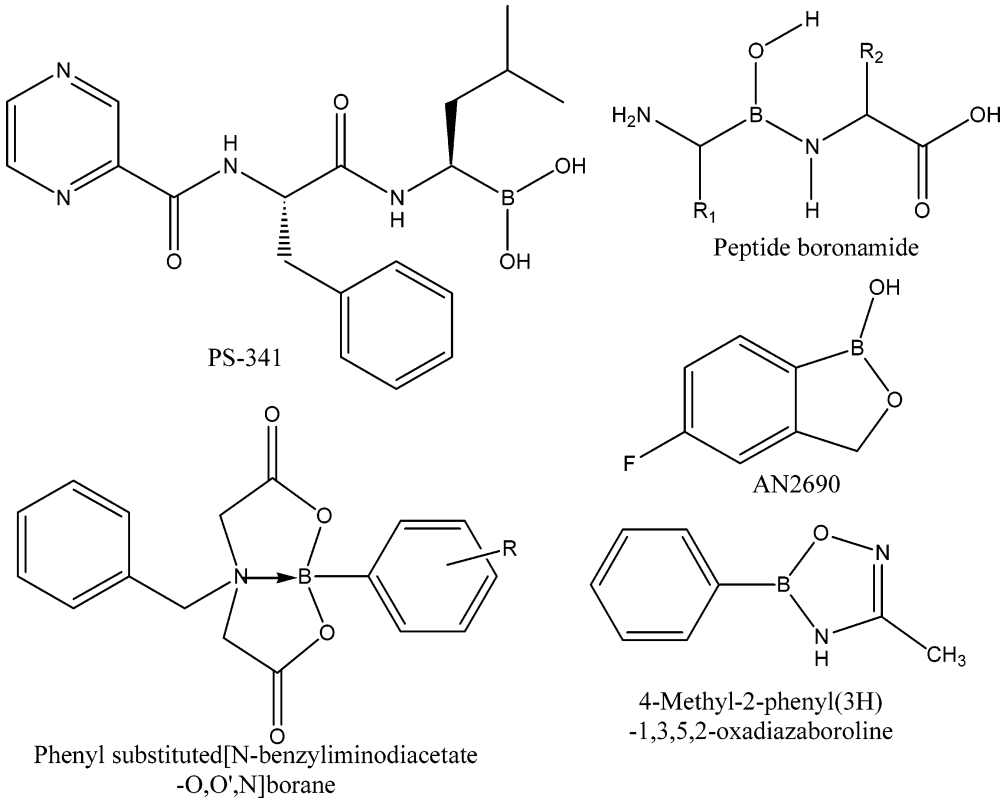

In previous papers, we had reported the effects on the structure, electronic properties, and conformation of peptides when the amide nitrogen is replaced by boron.[12−15] The peptide boronic acids [$NH_2-AA_n-B(OH)_2$], with the carbonyl group replaced by B−OH in the C-terminal end, have been reported in the literature as one of the most potent serine protease inhibitors. The potential applications of such peptides include the inhibition of thrombin, proteasome, dipeptidyl peptidase IV, chymotrypsin, leucocyte elastase, pancreatic elastase, hepatitis C virus NS3 protease, and penicillin-binding protein.[16] The X-ray crystallography and NMR studies on peptide boronic acids reveal that peptide boronic acid inhibitors analogous to the substrate form a tetrahedral boron−serine adduct in the active site, while other boronic acids form boron−histidine adducts in the active site of serine protease.[17] The dipeptide boronic acid PS-341[16] (Chart 1) is a potent inhibitor of proteasome and exhibits anti-inflammatory activity, while AN2690[16] (Chart 1), an organic boronic acid derivative, is a potent antifungal agent and is under clinical trial for the treatment of onychomycosis topical treatment.

Peptide boronic acids reported in the literature have been designed by replacing carbon by boron at the C-terminal end of the peptide. Replacement of the carbonyl group of a residue other than the C-terminal, by boron, leads to peptide boronamides (Chart 1). Close analogs of these molecules are known; for example, phenyl-substituted [*N*-benzyliminodiacetate-O,O′,N]boranes (Chart 1) has been designed as a cytotoxic and anticancer drug with potential applications in boron neutron capture therapy for the treatment of tumors and melanomas. Besides this, 4-methyl-2-phenyl(3H-)1,3,5,2-oxadiazoboroline (Chart 1) containing the boronamide moiety has been reported in the literature.[17]

We have investigated the geometry, conformation, and electronic properties of peptide boronamides (Chart 1) by ab initio and density functional methods. *N*-methylacetamide (NMA, Figure 1) is well-established as a model for natural peptides and proteins.[18] *N*-methyl-methylboronamide (NMB, Figure 1) constructed by replacing CO in NMA with B−OH serves as a simple model to analyze the preferences for the "ω angle" in peptide boronamides. The alanine analog (Ala-BON, Figure 1), derived from Ala-dipeptide (Figure 1), has been adopted as a model to study the ϕ and ψ preferences of peptide boronamides. The hypersurface of NMB, with its associated ground and transition states, and the ground states of Ala-BON have been mapped by ab initio Hartree−Fock

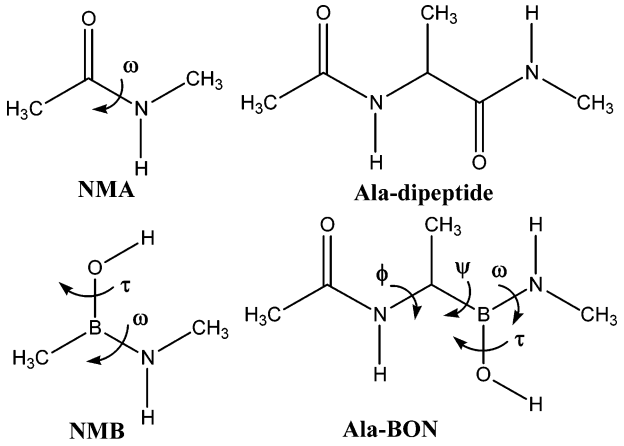

Figure 1. Structures of NMA, Ala-dipeptide, NMB, and Ala-BON.

Table 1. Energies (a.u.) and Relative Energies (kcal mol^{-1}) of Various Minima and Transition States on the PES of NMB at the HF, B3LYP, and MP2 Levels of Theory with the 6-31+G* Basis Set in the Aqueous Phase Using the PCM[a]

				HF/6-31+G*		B3LYP/6-31+G*		MP2(full)/6-31+G*			
		NIMAG	PG	a.u.[b]	rel.[c]	a.u.[b]	rel.[c]	a.u.[b]	rel.[c]	ω^d	τ^d
minima	GM	0	C_S	−234.3904417	0.0	−235.8715908	0.0	−235.109098	0.0	180	180
	LM1	0	C_S	−234.3898548	0.4	−235.8711296	0.3	−235.108948	0.1	0	180
	LM2	0	C_S	−234.3893319	0.7	−235.8706796	0.6	−235.107982	0.7	180	0
	LM3	0	C_S	−234.3879227	1.6	−235.8686787	1.8	−235.106071	1.9	0	0
ω rotation transition state (TS)	ωTS1	1	C_1	−234.3650603	15.9	−235.8455237	16.4	−235.082964	16.4	62/−62	−1
	ωTS2	1	C_1	−234.3621911	17.7	−235.8420428	18.5	−235.079209	18.8	113/−113	−1
	ωTS3	1	C_1	−234.3625781	17.5	−235.8427935	18.1	−235.079559	18.5	62/−62	179
	ωTS4	1	C_1	−234.3626095	17.5	−235.842479	18.3	−235.079838	18.4	118/−118	179
τ rotation TS	ωTS1	1	C_1	−234.3800096	6.5	−235.8611247	6.6	−235.097904	7.0	0	87/−87
	ωTS2	1	C_1	−234.3811566	5.8	−235.861951	6.0	−235.098847	6.4	183	88/−88

[a] NIMAG = number of imaginary frequency, PG = point group, GM = global minimum, LM = local minimum [b] Zero-point vibrational energy corrected values. [c] Relative energy in kcal mol^{-1}. [d] Torsion angle in degrees.

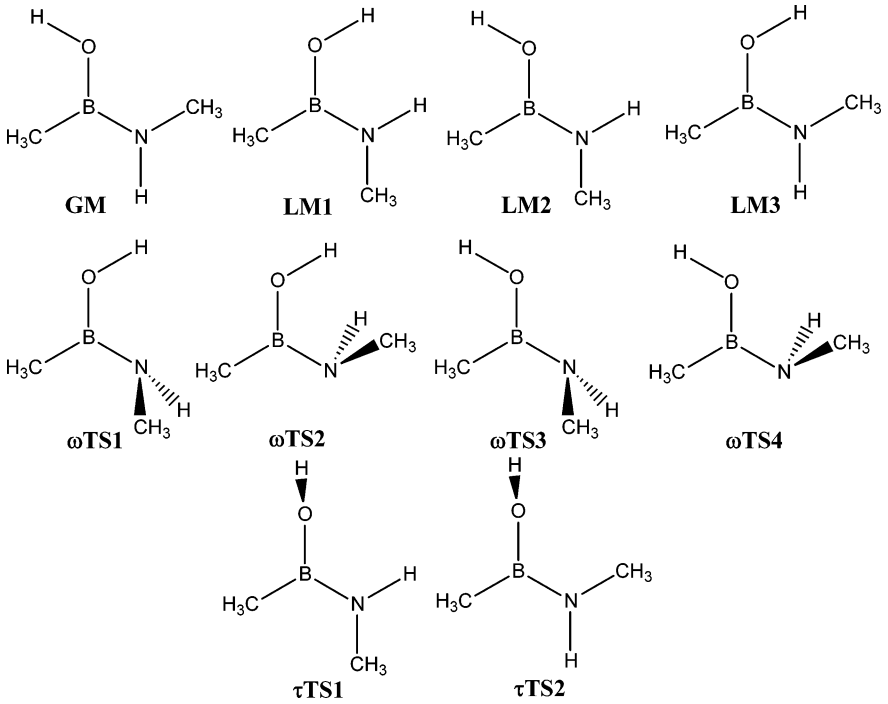

Figure 2. Structures of the minima and transition states on the PES of NMB.

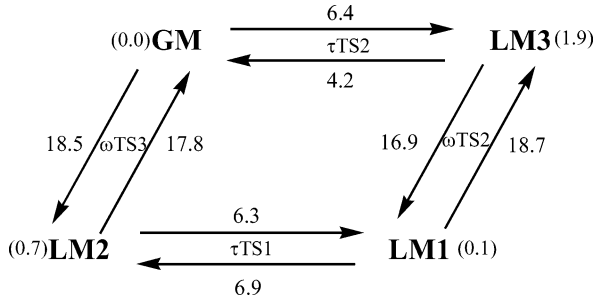

Figure 3. A schematic diagram showing interconversion between the various minima of NMB. The values on the arrows are energy barriers in kilocalories per mole, and the values in parentheses are relative energy values of minima in kilocalories per mole.

(HF), density functional, and post-HF methods. Second-order orbital interactions by the natural bond orbitals (NBO) method has also been carried out to understand the fundamental differences between the structures of peptide boronamides and their natural counterparts.

Computational Details

Ab initio molecular orbital[19] and density functional theory[20] calculations have been carried out with the Gaussian 03W (revision C.01)[21] package running on a 3.0 GHz Pentium IV processor with 1 GB of RAM. The stability of all wavefunctions was checked at the HF[22] and Becke's three-parameter exchange functional and the gradient-corrected functional of Lee, Yang, and Parr (B3LYP).[23] Second-order Møller−Plesset [MP2(full)][24] calculations were also carried out with the 6-31+G* basis set for all ground and transition state (TS) structures.

The two torsion angles, ω and τ, in *N*NMB are defined as shown in Figure 1. In NMB, the hydroxyl group can adopt two conformations around the B−O bond. In the first, the O−H bond is anti-periplanar with respect to the B−N bond, and the second arrangement is syn-periplanar. These initial

Table 2. Bond Length (Å) and Bond Angles (deg) of Minima and the TS of NMB Optimized at the MP2(full)/6-31+G* Level of Theory

parameter	GM	LM1	LM2	LM3	ω**TS1**	ω**TS2**	ω**TS3**	ω**TS4**	τ**TS1**	τ**TS2**
CB (1,2)	1.584	1.579	1.586	1.576	1.574	1.567	1.586	1.575	1.579	1.580
BO (2,3)	1.395	1.393	1.395	1.391	1.369	1.379	1.372	1.379	1.417	1.412
BN (2,4)	1.409	1.419	1.410	1.418	1.485	1.482	1.473	1.474	1.408	1.408
NC (4,5)	1.456	1.455	1.452	1.456	1.472	1.468	1.468	1.473	1.454	1.456
OH (3,6)	0.970	0.972	0.970	0.972	0.978	0.974	0.973	0.973	0.968	0.968
NH (4,7)	1.013	1.016	1.016	1.012	1.020	1.019	1.019	1.021	1.017	1.014
CBO (1,2,3)	121.4	116.4	122.4	116.8	118.3	117.4	121.4	122.4	118.3	119.5
CBN (1,2,4)	121.9	122.7	122.7	122.0	124.7	120.7	123.1	120.2	125.0	121.4
BOH (2,3,6)	112.3	114.2	112.6	114.2	108.1	112.2	112.2	112.8	116.5	116.9
BNC (2,4,5)	126.0	126.6	127.9	126.1	114.6	115.8	115.1	113.6	129.6	126.7
BNH (2,4,7)	118.8	120.0	117.0	118.6	111.6	114.3	112.5	111.0	115.9	118.4
CNH (5,4,7)	115.2	113.5	115.1	115.3	109.1	111.1	110.0	109.1	114.4	114.8
CBNC (ω) (1,2,4,5)	180.0	0.0	0.0	180.0	61.9/−61.9	114.0/−114.0	62.3/−62.3	118.8/−118.8	−0.3	−177.0
CBNH (1,2,4,7)	0.0	180.0	180.0	0.0	−62.6/62.6	−114.9/114.9	−64.9/64.9	−117.8/117.8	−175.7	0.9
NBOH (τ) (4,2,3,6)	180.0	0.0	180.0	0.0	−1.1	−1.3	179.2	178.8	87.0/−87.0	87.6/−87.6

Table 3. Partial Atomic Charges of NMB Calculated Using NPA and the "ESP Fit" as per the Merz−Singh−Kollman Scheme at the MP2(full)/6-31+G* Level and Using the PCM

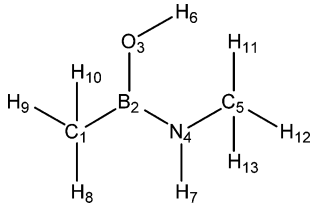

atom	ESP fitted charges	NPA charges
C1	−0.745	−1.040
B2	0.849	1.179
O3	−0.850	−1.044
N4	−0.809	−1.030
C5	0.183	−0.409
H6	0.493	0.557
H7	0.384	0.448
H8	0.139	0.234
H9	0.160	0.238
H10	0.160	0.238
H11	0.031	0.225
H12	−0.002	0.203
H13	−0.002	0.203

two conformations around the B−O bond in NMB were chosen, and for each arrangement of τ, a scan in increments of 30° of the "ω torsion angle" was carried out at the HF, B3LYP, and MP2(full) levels of theory using the 6-31+G* basis set. Conformations with the ω values of 0° and 180° were found to be the lowest in energy. Now, for each conformation with a ω value of 0° or 180°, a τ scan in increments of 30° was run at the HF, B3LYP, and MP2-(full) levels of theory with the 6-31+G* basis set. The minima and saddle points for rotations about the ω and τ torsions were thus identified. All these conformations were further optimized, without constraints, at the B3LYP and MP2 levels of theory with the same basis set, and finally, the energies of the optimized structures were further calculated in the aqueous phase using the self-consistent reaction field (SCRF) polarizable continuum model (PCM). The stable conformations were confirmed by frequency calculations, which returned one imaginary frequency for each transition state and all positive frequencies for each ground state.

The NBO[25] analysis was carried out on the global minimum energy structure (GM) of NMB, optimized at the MP2(full)/6-31+G* level, to quantitatively estimate the second-order interactions as $E_{ij} = -2F_{ij}/\Delta E_{ij}$, where E_{ij} is the energy of the second-order interaction, $\Delta E_{ij} = E_i - E_j$ is the energy difference between the interacting molecular orbitals i and j, and F_{ij} is the Fock matrix element for the interaction between orbitals i and j. The "atomic partial charges" of the global minimum of NMB, optimized at the MP2(full)/6-31+G* level, were calculated using natural population analysis (NPA) as implemented in NBO and additionally by the "ESP fit" method formulated by Merz et al.[26]

For Ala-BON, the minima in the ϕ and ψ space was searched starting with the four different conformations for ω and τ identified (Table 1) previously for NMB. This corresponds to structures (i) $\omega = 180°$, $\tau = 180°$; (ii) $\omega = 0°$, $\tau = 180°$; (iii) $\omega = 180°$, $\tau = 0°$; and (iv) $\omega = 0°$, $\tau = 0°$ labeled as Ala-BON1, Ala-BON2, Ala-BON3, and Ala-BON4, respectively. For each (ω,τ) combination, 144 conformations were generated with 30° increments of the ϕ and ψ dihedrals. Each conformation was geometry-optimized first at the HF/3-21G level of theory with "constraints" on the initial ϕ and ψ angles. A Ramachandran map of the 144 conformations was constructed, and conformations within 10.0 kcal mol^{-1} of the global minimum were identified. These low-energy conformations were further optimized without constraints at the B3LYP/6-31+G* level of theory in the aqueous phase using the SCRF PCM.

Results and Discussion

All wavefunctions for molecules NMB and Ala-BON were found to be stable under the perturbations considered at the HF, B3LYP, and MP2 levels of theory.

Minima and Saddle Points of NMB. The conformations of the minima and various transition states for NMB are

Table 4. Torsion Angles (in degrees), Relative Energies (kcal mol^{-1}), and Secondary Structure Features of Minima of Ala-BON

	ω	τ	ϕ	ψ	rel. E (kcal mol^{-1})	structural feature (ideal values of the torsion angles)
Ala-BON1	180	180	61	129	0.0	type II′ β turn, second residue (60,120), positive ϕ
			−74	−122	0.9	type II β turn, second residue (−60,−120)
Ala-BON2	0	180	62	132	0.0	type II′ β turn, second residue (60,120), positive ϕ
Ala-BON3	180	0	−141	135	0.0	antiparallel β sheet (−139,135)
			68	−46	4.2	mirror image of 2.27 ribbon (78,−59), positive ϕ
Ala-BON4	0	0	−144	154	0.0	antiparallel β sheet (−139,135)
			−57	−46	1.7	α helix (−57,−47)

depicted in Figure 2, and their absolute and relative energies at the HF, B3LYP, and MP2(full) levels of theory with the 6-31+G* basis set and the PCM are given in Table 1. For NMB, besides the GM, there exist three local minima (LM1, LM2, and LM3). These local minima occur respectively at 0.1, 0.7, and 1.9 kcal mol^{-1} above the global minimum. Depending upon the pyramidal state of nitrogen (i.e., "pyramidal up" or "pyramidal down") and the relative orientation of the hydroxyl group (i.e., "τ angle"), there exist four transition states for rotation around the "ω angle" (ωTS1 to ωTS4). The natural peptide NMA exhibits two minima (global and local) and two transition states for the rotation around the "ω angle'.[27] The minima and transition states of NMB closely parallel those of NMA, with the exception that two additional minima and two additional transition states for rotation around the "ω angle" appear. This is a consequence of the hydroxyl group, which is absent in NMA. There are two transition states for rotation around the "τ angle", namely, τTS1 and τTS2. All minima of NMB exhibit C_S symmetry while the transition states have C_1 symmetry. The GM has $\omega = 180°$ and $\tau = 180°$, like the GM of NMA with $\omega = 180°$ and C_S symmetry.

Figure 3 depicts the interconversion between the four minima of NMB and the associated energy barriers. Although all three local minima lie within 2.0 kcal mol^{-1} of the global minimum, the barriers for interconversions are relatively high. The lowest barrier at 4.2 kcal mol^{-1} is associated with the conversion of LM3 to GM. The conversion of LM1 to LM3 has the highest barrier of 18.7 kcal mol^{-1}. The GM ↔ LM3 and LM1 ↔ LM2 interconversions exhibit relatively low energy barriers, while the GM ↔ LM2 and LM1 ↔ LM3 interconversions involve higher energy barriers. The interconversion between GM ↔ LM1 and LM2 ↔ LM3 follows a two-step process or involves a saddle point of index 2.

The geometric parameters of the minima and the transition states of NMB at the MP2(full)/6-31+G* level of theory are given in Table 2. There is a small increase of about 0.06−0.07 Å in the B−N bond length in the transition states for rotation about the "ω angle" compared to the ground states. Crystallographic data is available for a large number of "organic boronic acids" [R−B(OH)$_2$] and "peptide boronic acids" [AA−CONH−C(R)H−B(OH$_2$)], but no experimental data are yet available for boronamides. However, the crystal structure[28] of a cyclic boron derivative, 4-methyl-2-phenyl-(3H)-1,3,5,2-oxadiazaboroline (Chart 1), which is related to NMB has been reported. The B−O bond length in NMB is found to be 1.391−1.395 Å (Table 2) at the MP2(full)/6-31+G* level of theory. In comparison, the B−O bond length, reported in the literature for a range of organic and inorganic boron-containing molecules, varies from 1.34 to 1.42 Å (average 1.38 Å) for boron with trigonal planar geometry and 1.39 to 1.52 Å (average 1.48 Å) for boron with tetrahedral geometry.[29] In 4-methyl-2-phenyl-(3H)-1,3,5,2-oxadiazaboroline, the B−O bond length is 1.39 Å. Similarly, the B−N bond length of NMB is found to be 1.409−1.419 Å, while that in 4-methyl-2-phenyl-(3H)-1,3,5,2-oxadiazaboroline is 1.41 Å. The B−O and B−N bond lengths signify appreciable π character for these bonds. The C−B bond length of NMB is found to be 1.576−1.586 Å, while that in 4-methyl-2-phenyl-(3H)-1,3,5,2-oxadiazaboroline is 1.56 Å. In alkylboranes, the B−C (aliphatic carbon) bond length is about 1.590 Å, as is that for, for example, dimethylborane,[30] and it is 1.596 Å in dimesitylborane,[31] 1.570 Å in ditripylborane,[32] 1.571 Å in BMA (acetylmethylborane),[13] 1.564 Å in BMAOH (acetylmethylhydroxyborane),[14] and 1.612 Å in BMA−BOM (acetylmethylmethoxyborane).[15] The bond lengths for NMB calculated in this study are in the range of the experimental values for related compounds.

Rotation Barriers in NMB. The barrier to rotation about the "ω angle" in the natural peptide ranges from 16.0 to 25.0 kcal mol^{-1}. The "ω rotation" barrier in NMB at the MP2-(full)/6-31+G* level of theory is found to be 16.4−18.8 kcal mol^{-1}, which is comparable to the value in natural peptides. In sharp contrast, replacement of the nitrogen of the amide group by boron leads to a lowering (∼5.0 kcal mol^{-1}) of the "ω rotation" barrier in boron peptides.[13] The results of the NBO study reveal that the energy $E^{(2)}$ associated with $n_O \rightarrow \pi^*_{B-N}$ interaction (delocalization from lone pairs on oxygen into the π antibonding orbital of the B−N bond) is 51.4 kcal mol^{-1} and that for the $n_O \rightarrow \sigma^*_{B-N}$ interaction (delocalization from lone pairs on oxygen into the σ antibonding orbital of the B−N bond, i.e., negative hyperconjugation) is 3.6 kcal mol^{-1} in the GM of NMB at the MP2(full)/6-31+G* level of theory. In comparison, the energy associated with negative hyperconjugation, that is, $n_O \rightarrow \sigma^*_{C-N}$, is 32.8 kcal mol^{-1}, and that for $n_N \rightarrow \pi^*_{C-O}$ is 98.5 kcal mol^{-1} for the global energy minimum structure of NMA.[13] These two interactions are responsible for the high barrier to rotation about the C−N and the B−N bonds in NMA and NMB, respectively. The NBO analysis also yields a bond order of 2 for the B−N bond in NMB, which also explains the existence of the high ω rotation barrier in NMB. The barrier to τ rotation (B−O bond) in NMB is found to

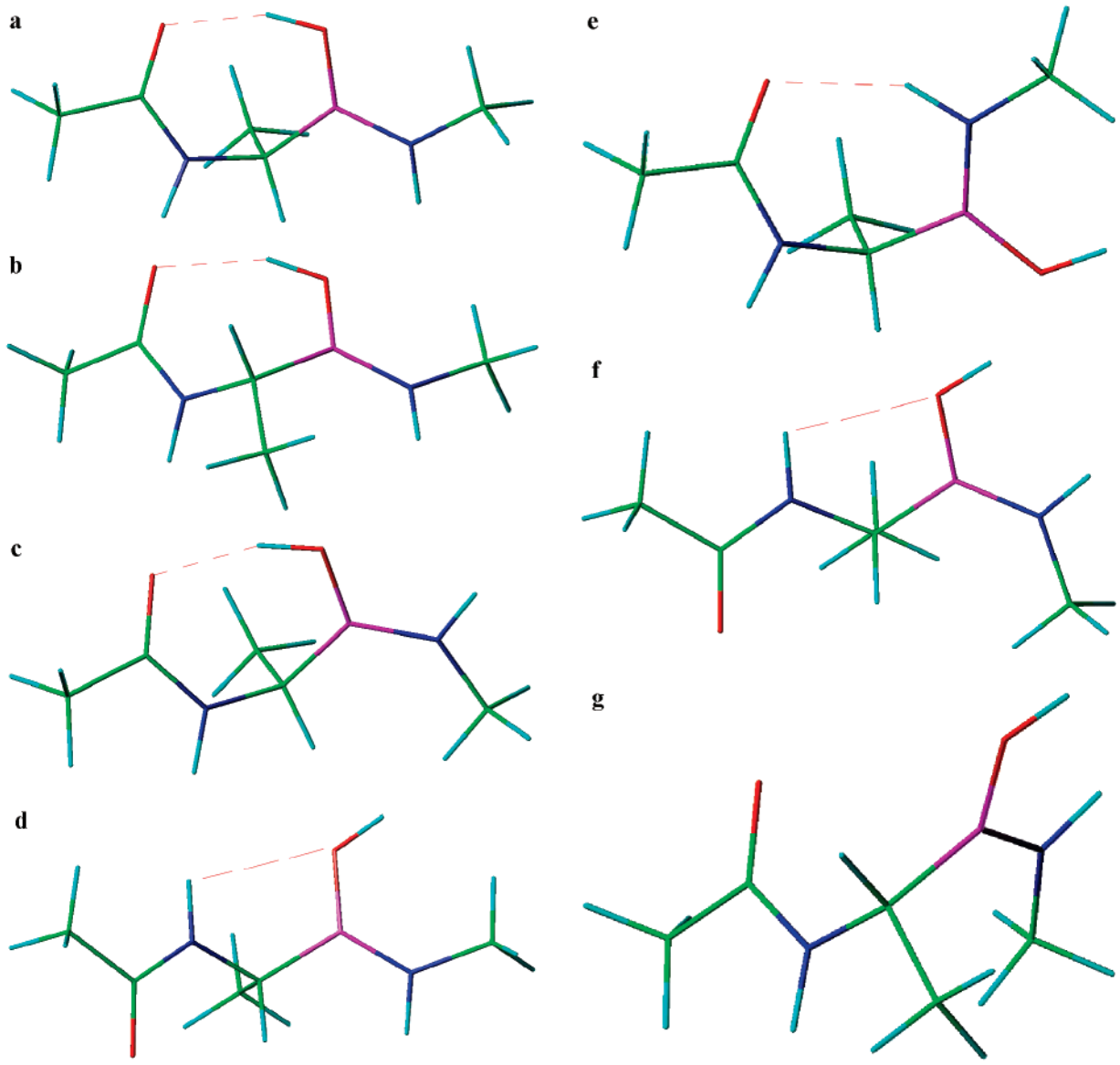

Figure 4. Preferred conformations of Ala-BON. Ala-BON1: (a) $\omega = 180°$, $\tau = 180°$, $\phi = 61°$, $\psi = 129°$ and (b) $\omega = 180°$, $\tau = 180°$, $\phi = -74°$, $\psi = -122°$. Ala-BON2: (c) $\omega = 0°$, $\tau = 180°$, $\phi = 62°$, $\psi = 132°$. Ala-BON3: (d) $\omega = 180°$, $\tau = 0°$, $\phi = -141°$, $\psi = 135°$ and (e) $\omega = 180°$, $\tau = 0°$, $\phi = 68°$, $\psi = -46°$. Ala-BON4: (f) $\omega = 0°$, $\tau = 0°$, $\phi = -144°$, $\psi = 154°$ and (g) $\omega = 0°$, $\tau = 0°$, $\phi = -57°$, $\psi = -46°$. Atom color codes: carbon, green; nitrogen, blue; oxygen, red; boron, magenta; hydrogen, cyan.

be between 6.4 and 7.0 kcal mol^{-1} at the MP2(full)/6-31+G* level of theory. The NBO results indicate a single bond for B−O, which is in line with the relatively low rotation barrier.

Partial Atomic Charges of NMB. The "natural charges" derived from NPA and ESP-fitted charges as per the Merz−Singh−Kollman scheme for the global minimum energy structure of NMB are listed in Table 3. The large positive charge on boron will make it the favored site for a nucleophilic attack leading ultimately to the formation of a stable tetrahedral adduct. The boronamides thus follow a chemistry similar to that of the peptide boronic acids, which are potent inhibitors of serine protease.[16] The peptide boronamides are therefore expected to act as strong inhibitors of serine protease.

Potential Energy Surface (PES) of Ala-BON. The four minima of NMB for the ω and τ torsions give rise to four different starting structures (Ala-BON1 to -4), whose minima in the ϕ and ψ space were scanned (Table 4). In Ala-BON1, with an ω value of 180° and a τ value of 180°, the global minimum corresponds to a structure with $\phi = 61°$ and $\psi = 129°$ (Figure 4a). These values are close to those for the second residue in a type-II′ β turn (ideal values $\phi = 60°$ and $\psi = 120°$). The local minimum energy structure with $\phi = -74°$ and $\psi = -122°$ (Figure 4b) corresponds to a β turn of type II (ideal values $\phi = -60°$ and $\psi = -120°$). In Ala-BON2, with an ω value of 0° and a τ value of 180°, there is only the global minimum energy structure with $\phi = 62°$ and $\psi = 132°$ (Figure 4c), which is very similar to the global minimum of Ala-BON1 with regard to τ, ϕ, and ψ angles but with a difference in the "ω angles". Both structures exhibit a positive ϕ value which is not favored by natural peptides. All minima of Ala-BON1 and Ala-BON2 have an intramolecular hydrogen bond (Figure 4a−c) between the

carbonyl O atom (acting as an acceptor) and the OH group attached to boron (acting as a donor).

Ala-BON3, with an ω value of 180° and a τ value of 0°, has one local minimum within 10.0 kcal mol^{-1} of the global minimum structure. The global minimum is a structure with $\phi = -141°$ and $\psi = 135°$ (Figure 4d) corresponding to an antiparallel β sheet (ideal values $\phi = -139°$ and $\psi = 135°$). The local minimum is a structure with $\phi = 68°$ and $\psi = -46°$ (Figure 4e) which is close to a 2.27 ribbon structure (ideal $\phi = -78°$ and $\psi = 59°$), and the ϕ value falls in the "disallowed region" of the Ramachandran map. The global minimum of Ala-BON3 exhibits a hydrogen bond (Figure 4d) between the amide N atom (acting as an acceptor) and the OH group attached to boron (acting as a donor). The local minimum structure has a hydrogen bond (Figure 4e) between the carbonyl O atom (acting as an acceptor) and the NH group attached to boron (acting as a donor).

The last structure, Ala-BON4, with an ω value of 180° and a τ value of 0°, also has one local minimum within 10.0 kcal mol^{-1} of the global minimum structure. The global minimum corresponds to a structure with $\phi = -144°$ and $\psi = -154°$ (Figure 4f) and resembles an antiparallel β sheet ($\phi = -139°$, $\psi = 135°$). The local minimum is a structure with $\phi = -57°$ and $\psi = -46°$ (Figure 4g), and these values are for an α helix ($\phi = -57°$, $\psi = -47°$). In Ala-BON4, only the global minimum displays a hydrogen bond (Figure 4f) between the amide N atom (acting as an acceptor) and the OH group attached to boron (acting as a donor).

The conformational preferences of natural peptides are governed by their ϕ and ψ values, which often lie within the "allowed regions" of the Ramachandran map. The replacement of CO by B−OH in natural peptides leads to structures with regular secondary motifs, in addition to few secondary structures with "disfavored" positive ϕ values, for, for example, mirror images of the type-II β-turn and the 2.27 ribbon motifs.

Conclusions

A novel boron analog of peptides has been designed by replacing the amide (CO−NH) moiety with the B(OH)−NH group. To understand the geometrical properties of these analogs around the ω angle, NMB has been established as a model peptide. The PES of NMB is characterized by four minima, four TSs for rotation around the "ω angle", and two TSs for rotation about the τ angle. The barriers for rotation about the "ω angle" are in the range of 16.4−18.8 kcal mol^{-1}, and those for rotation about the τ angle are 6.4−7.0 kcal mol^{-1}. The NBO study reveals that the B−N bond has appreciable double-bond character, and single-bond character for the B−O bond, which explains the relative differences in the rotation barriers of the ω and τ angles. The "ω angle" and its associated rotation barrier are remarkably similar to the corresponding values of natural peptides. The Ala-dipeptide derived from NMB favors α-helix, type-II β-turn, 2.27 ribbon, and antiparallel β-sheets conformations and structures which are mirror images of the type-II β-turn and the 2.27 ribbon motifs. These latter structures fall in the "disallowed regions" of the Ramachandran map. In conclusion, the replacement of CO by B−OH in peptides retains the backbone geometry in a trans configuration. This makes the B−OH moiety a good surrogate for the CO group in peptides, with the additional property that such analogs will be resistant to hydrolytic cleavage by the enzymes—amidases and peptidases.

Acknowledgment. This work is supported by the Department of Science and Technology (DST), New Delhi, through their FIST program (SR/FST/LS1−163/2003). A.K.M. and S.A.K. thanks the Council of Scientific and Industrial Research (CSIR), New Delhi, financial support.

References

(1) Gante, J. Peptidomimetics − Tailor-Made Enzyme Inhibitors. *Angew. Chem., Int. Ed. Engl.* **1994**, *33*, 1699−1720.

(2) Hruby, V. J. Designing Peptide Receptor Agonists and Antagonists. *Nat. Rev. Drug Discovery* **2002**, *1*, 847−858.

(3) Fischer, P. M. The Design, Synthesis and Application of Stereochemical and Directional Peptide Isomers: A Critical Review. *Curr. Protein Pept. Sci.* **2003**, *4*, 339−356.

(4) Thormann, M.; Hoffmann, H. J. Conformational Properties of Peptides Containing Dehydro Amino Acids. *THEOCHEM* **1998**, *431*, 79−96.

(5) Mohle, K.; Hoffmann, H. J. Secondary Structure Formation in N-Substituted Peptides. *J. Pept. Res.* **1998**, *51*, 19−28.

(6) (a) Cheng, R. P.; Gellman, S. H.; DeGrado, W. F. Beta-Peptides: From Structure to Function. *Chem. Rev.* **2001**, *101*, 3219−3232. (b) Hanessian, S.; Luo, X. H.; Schaum, R.; Michnick, S. Design of Secondary Structures in Unnatural Peptides − Stable Helical γ-Tetra-, Hexa- and Octapeptides and Consequences of α-Substitution. *J. Am. Chem. Soc.* **1998**, *120*, 8569−8570. (c) Grison, C.; Geneve, S.; Coutrot, P. Enantioselective Synthesis of α,β-Unsaturated γ- and δ-Lactams. *Tetrahedron Lett.* **2001**, *42*, 3831−3834.

(7) (a) Cho, C. Y.; Moran, E. J.; Cherry, S. R.; Stephans, J. C.; Fodor, S. P. A.; Adams, C. L.; Sundaram, A.; Jacobs, J. W.; Schultz, P. G. An Unnatural Biopolymer. *Science* **1993**, *261*, 1303−1305. (b) Rushing, S. D.; Hammer, R. P. Synthesis of Phosphonamide and Thiophosphonamide Dipeptides. *J. Am. Chem. Soc.* **2001**, 123, 4861−4862. (c) Baldauf, C.; Günther, R.; Hoffmann, H. J. Conformational Properties of Sulfonamido Peptides. *THEOCHEM* **2004**, *675*, 19−28.

(8) Cervini, L.; Theobald, P.; Corrigan, A.; Craig, A. G.; Rivier, C.; Vale, W.; Rivier, J. Corticotropin Releasing Factor (CRF) Agonists with Reduced Amide Bonds and Ser7 Substitutions. *J. Med. Chem.* **1999**, *42*, 761−768.

(9) Vogen, S. M.; Paczkowski, N. J.; Kirnarsky, L.; Short, A.; Whitmore, J. B.; Sherman, S. A.; Taylor, S. M.; Sanderson, S. D. Differential Activities of Decapeptide Agonists of Human C5a: The Conformational Effects of Backbone *N*-Methylation. *Int. Immunopharmacol.* **2001**, *12*, 2151−2162.

(10) Ye, Y.; Liu, M.; Kao, J. L.; Marshall, G. R. Peptide-Bond Modification for Metal Coordination: Peptides Containing Two Hydroxamate Groups. *Biopolymers* **2003**, *71*, 489−515.

(11) (a) Spielvogel, B. F.; Das, M. K.; McPhail, A. T.; Onam, K. D.; Hall, I. H. Boron Analogs of the α-Amino Acids. Synthesis, X-Ray Crystal Structure, and Biological Activity of Ammonia-Carboxyborane, the Boron Analog of Glycine.

J. Am. Chem. Soc. **1980**, *102*, *6343*−6344. (b) Miller, M. C.; Sood, A.; Spielvogel, B. F.; Hall, I. H. Synthesis and Antitumor Activity of Boronated Dipeptides Containing Aromatic Amino Acids. *Anticancer Res.* **1997**, *5A*, 3299−3306.

(12) Datar, P. A.; Coutinho, E. C. The ϕ, ψ Space of Boron Isosteres of Amino Acids: An *ab Initio* Study. *J. Theor. Comput. Chem.* **2004**, *3*, 189−202.

(13) Malde, A. K.; Khedkar, S. A.; Coutinho, E. C.; Saran, A. Geometry, Transition States, and Vibrational Spectra of Boron Isostere of *N*-Methylacetamide by ab Initio Calculations. *Int. J. Quantum Chem.* **2005**, *102*, 734−742.

(14) Malde, A. K.; Khedkar, S. A.; Coutinho, E. C. The ω, ϕ and ψ Space of *N*-Hydroxy-*N*-methylacetamide and *N*-Acetyl-*N*′-hydroxy-*N*′-methylamide of Alanine and Their Boron Isosteres. *J. Chem. Theory Comput.* **2006**, *2*, 312−321.

(15) Malde, A. K.; Khedkar, S. A.; Coutinho, E. C. The Stationary Points of the PES of N-Methoxy Peptides and Their Boron Isosteres: An *ab Initio* Study. *J. Chem. Theory Comput.* **2006**, *2*, 1664−1674.

(16) (a) Kettner, C.; Mersinger, L.; Knabb, R. The Selective Inhibition of Thrombin by Peptides of Boroarginine. *J. Biol. Chem.* **1990**, *265*, 18289−18297. (b) Archer, S. J.; Camac, D. M.; Wu, Z. J.; Farrow, N. A.; Domaille, P. J.; Wasserman, Z. R.; Bukhtiyarova, M.; Rizzo, C.; Jagannathan, S.; Mersinger, L. J.; Kettener, C. A. Hepatitis C Virus NS3 Protease Requires Its NS4A Cofactor Peptide for Optimal Binding of a Boronic Acid Inhibitor as Shown by NMR. *Chem. Biol.* **2002**, *9*, 79−92. (c) Pargellis, C. A.; Campbell, S. J.; Pav, S.; Graham, E. T.; Pitner, T. P. Inhibition of Dipeptidyl Petidase IV (CD26) by Peptide Boronic Acid Dipeptides. *J. Enzyme Inhib.* **1997**, *11*, 151−169. (d) Nicola, G.; Peddi, S.; Stefanova, M.; Nicholas, R. A.; Gutheil, W. G.; Davies, C. Crystal Structure of Escherichia coli PBP 5 Bound to a Tripeptide Boronic Acid Inhibitor: A Role for Ser110 in Deacylation. *Biochemistry* **2005**, *44*, 8207−8217. (e) Richardson, P. G.; Mitsiades, C.; Hideshima, T.; Anderson, K. C. Proteasome Inhibition in the Treatment of Cancer. *Cell Cycle* **2005**, *4*, 290−296. (f) Priestley, E. S.; De Lucca, I.; Ghavimi, B.; Erickson-Viitanen, S.; Decicco, C. P. P1 Phenethyl Peptide Boronic Acid Inhibitors of HCV NS3 Protease. *Bioorg. Med. Chem. Lett.* **2002**, *12*, 3199−3202. (g) Tapparelli, C.; Metternich, R.; Ehrhardt, C.; Zurini, M.; Claeson, G.; Scully, M. F.; Stone, S. R. In Vitro and in Vivo Characterization of a Neutral Boron-Containing Thrombin Inhibitor. *J. Biol. Chem.* **1993**, *268*, 4734−4741. (h) Soskel, N. T.; Watanabe, S.; Hardie, R.; Shenvi, A. B.; Punt, J. A.; Kettner, C. A New Peptide Boronic Acid Inhibitor of Elastase-Induced Lung Injury in Hamsters. *Am. Rev. Respir. Dis.* **1986**, *133*, 639−642. (i) Palombella, V. J.; Conner, E. M.; Fuseler, J. W.; Destree, A.; Davis, J. M.; Laroux, F. S.; Wolf, R. E.; Huang, J.; Brand, S.; Elliott, P. J.; Lazarus, D.; McCormack, T.; Parent, L.; Stein, R.; Adams, J.; Grisham, M. B. Role of the Proteasome and NF-kB in Streptococcal Cell Wall-Induced Polyarthritis. *Proc. Natl. Acad. Sci. U.S.A.* **1998**, *95*, 15671−15676. (j) Baker, S. J.; Zhang, Y. K.; Akama, T.; Lau, A.; Zhou, H.; Hernandez, V.; Mao, W.; Alley, M. R. K.; Sanders, V.; Plattner, J. J. Discovery of a New Boron-Containing Antifungal Agent, 5-Fluoro-1,3-dihydro-1-hydroxy-2,1-benzoxaborole (AN2690), for the Potential Treatment of Onychomycosis. *J. Med. Chem.* **2006**, *49*, 4447−4450.

(17) (a) Farr-Jones, S.; Smith, S. O.; Kettner, C. A.; Griffin, R. G.; Bachovchin, W. W. Crystal versus Solution Structure of Enzymes: NMR Spectroscopy of a Peptide Boronic Acid-Serine Protease Complex in the Crystalline State. *Proc. Natl. Acad. Sci. U.S.A.* **1989**, *86*, 6922−6924. (b) Ivanov, D.; Bachovchin, W. W.; Redfield, A. G. Boron-11 Pure Quadrupole Resonance Investigation of Peptide Boronic Acid Inhibitors Bound to Alpha-Lytic Protease. *Biochemistry* **2002**, *41*, 1587−1590. (c) Davis, J. H.; Agard, D. A.; Handel, T. M.; Basus, V. J. Alterations in Chemical Shifts and Exchange Broadening upon Peptide Boronic Acid Inhibitor Binding to Alpha-Lytic Protease. *J. Biomol. NMR* **1997**, *10*, 21−27. (d) Tsilikounas, E.; Kettner, C. A.; Bachovchin, W. W. Boron-11 NMR Spectroscopy of Peptide Boronic Acid Inhibitor Complexes of α-Lytic Protease. Direct Evidence for Tetrahedral Boron in Both Boron-Histidine and Boron-Serine Adduct Complexes. *Biochemistry* **1993**, *32*, 12651−12655. (e) Mancilla, T.; Zamudio-Rivera, L. S.; Hiram; Beltran, I.; Santillan, R.; Farfan, N. Synthesis and Characterization of New (N→*B)* Phenyl Substituted [N-Benzyliminodiacetate-O,O′,N]boranes. *ARKIVOC (Gainesville, FL, U.S.)* **2005**, *6*, 366−376.

(18) Shipman, L. L.; Christoffersen, R. E. Ab Initio Calculations on Large Molecules Using Molecular Fragments. Model Peptide Studies. *J. Am. Chem. Soc.* **1973**, *95*, 1408−1416.

(19) Hehre, W. J.; Random, L.; Schlyer, P. V. R.; Pople, J. *Ab Initio Molecular Orbital Theory*; Wiley: New York, 1985.

(20) Parr, R. G.; Yang, W. *Density Functional Theory of Atoms and Molecules*; O.U.P.: New York, 1989.

(21) Frisch, M. J.; Trucks, G. W.; Schlegel, H. B.; Scuseria, G. E.; Robb, M. A.; Cheeseman, J. R.; Montgomery, J. A., Jr.; Vreven, T.; Kudin, K. N.; Burant, J. C.; Millam, J. M.; Iyengar, S. S.; Tomasi, J.; Barone, V.; Mennucci, B.; Cossi, M.; Scalmani, G.; Rega, N.; Petersson, G. A.; Nakatsuji, H.; Hada, M.; Ehara, M.; Toyota, K.; Fukuda, R.; Hasegawa, J.; Ishida, M.; Nakajima, T.; Honda, Y.; Kitao, O.; Nakai, H.; Klene, M.; Li, X.; Knox, J. E.; Hratchian, H. P.; Cross, J. B.; Adamo, C.; Jaramillo, J.; Gomperts, R.; Stratmann, R. E.; Yazyev, O.; Austin, A. J.; Cammi, R.; Pomelli, C.; Ochterski, J. W.; Ayala, P. Y.; Morokuma, K.; Voth, G. A.; Salvador, P.; Dannenberg, J.; Zakrzewski, V. G.; Dapprich, S.; Daniels, A. D.; Strain, M. C.; Farkas, O.; Malick, D. K.; Rabuck, A. D.; Raghavachari, K.; Foresman, J. B.; Ortiz, J. V.; Cui, Q.; Baboul, A. G.; Clifford, S.; Cioslowski, J.; Stefanov, B. B.; Liu, G.; Liashenko, A.; Piskorz, P.; Komaromi, I.; Martin, R. L.; Fox, D. J.; Keith, T.; Al-Laham, M. A.; Peng, C. Y.; Nanayakkara, A.; Challacombe, M.; Gill, P. M. W.; Johnson, B.; Chen, W.; Wong, M. W.; Gonzalez, C.; Pople, J. A. *Gaussian 03*, revision C.01; Gaussian, Inc.: Wallingford, CT, 2004.

(22) Roothan, C. C. New Developments in Molecular Orbital Theory. *Rev. Mod. Phys.* **1951**, *23*, 69−89.

(23) (a) Becke, A. D. Density Functional Thermochemistry. III. The Role of Exact Exchange. *J. Chem. Phys.* **1993**, *98*, 5648−5652. (b) Lee, C.; Yang, W.; Parr, R. G. Development of the Colle-Salvetti Correlation-Energy Formula into a Functional of the Electron Density. *Phys. Rev. B: Condens. Matter Mater. Phys.* **1988**, *37*, 785−789. (c) Perdew, J. P.; Wang, Y. Accurate and Simple Analytic Representation of the Electron-Gas Correlation Energy. *Phys. Rev. B: Condens. Matter Mater. Phys.* **1992**, *45*, 13244−13249.

(24) (a) Møller, C.; Plesset, M. S. Note on an Approximation Treatment for Many-Electron Systems. *Phys. Rev.* **1934**, *46*, 618−622. (b) Martin-Head, G.; Pople, J. A.; Frisch, M. J. MP2 Energy Evaluation by Direct Methods. *Chem. Phys. Lett.* **1988**, *153*, 503−506.

(25) (a) Glendening, E. D.; Reed, A. E.; Carpenter, J. E.; Weinhold, F. *NBO*, version 3.1. (b) Reed, A. E.; Weinstock, R. B.; Weinhold, F. Natural Population Analysis. *J. Chem. Phys.* **1985**, *83*, *735*−746. (c) Reed, A. E.; Weinhold, F.; Curtiss, L. A. Intermolecular Interactions from a Natural Bond Orbital, Donor-Acceptor Viewpoint. *Chem. Rev.* **1988**, *88*, 899−926.

(26) Singh, U. C.; Kollman, P. A. An Approach to Computing Electrostatic Charges for Molecules. *J. Comput. Chem.* **1984**, *5*, 129−145.

(27) Villani, V.; Alagona, G.; Ghio, C. Ab Initio Studies on N-Methylacetamide. *Mol. Eng.* **1999**, *8*, 135−153.

(28) Raper, E. S. The Crystal and Molecular Structure of 4-Methyl-2-phenyl-(3H)-1,3,5,2-oxadiazaboroline. *Acta Crystallogr., Sect. B* **1978**, *34*, 3281−3284.

(29) (a) Filatov, S.; Shepelev, Y.; Bubnova, R.; Sennova, N.; Egorysheva, A. V.; Kargin, Y. F. The Study of $Bi_3B_5O_{12}$: Synthesis, Crystal Structure and Thermal Expansion of Oxoborate $Bi_3B_5O_{12}$. *J. Solid State Chem.* **2004**, *177*, 515−522. (b) Shishkov, I. F.; Khristenko, L. V.; Rudakov, F. M.; Vilkov, L. V.; Karlov, S. S.; Zaitseva, G. S.; Samdal, S. The Molecular Structure of Boratrane Determined by Gas Electron Diffraction and Quantum Mechanical Calculations. *J. Mol. Struct.* **2002**, *641*, 199−205.

(30) Vijay, A.; Sathyanarayana, D. N. Effects of Basis Set and Electron Correlation on the Structure and Vibrational Spectra of Diborane. *J. Mol. Struct.* **1995**, *351*, 215−229.

(31) Entwistle, C. D.; Marder, T. B.; Smith, P. S.; Howard, A. K.; Fox, M. A.; Mason, S. A. Dimesitylborane Monomer−Dimer Equilibrium in Solution, and the Solid-State Structure of the Dimer by Single Crystal Neutron and X-ray Diffraction. *J. Organomet. Chem.* **2003**, *680*, 165−172.

(32) Bartlett, R. A.; Rasikadis, H. V.; Olmstead, M. M.; Power, P. P.; Weese, K. J. Synthesis of the Monomeric $HBtrip_2$ (trip = 2,4,6-iso-$Pr_3C_6H_2$) and the X-ray Crystal Structures of $[HBMes_2]_2$ (Mes = 2,4,6,-$Me_3C_6H_2$) and $HBtrip_2$. *Organometallics* **1990**, *9*, 146−150.

CT600256S